Equilibration Processes of Quantum Many-Neutrino Systems in Core-Collapse Supernovae

Student: Nikoli Ralph[1]
Mentors: Vincenzo Cirigliano[1] and Yukari Yamauchi[1]
[1]Institute for Nuclear Theory, University of Washington, Seattle, WA 98195, USA

September 6, 2025

Abstract

Accurately modeling dense neutrino systems is critical to the understanding of high density astrophysical environments, such as core-collapse supernovae and neutron star mergers. In this project, we investigate how the number of neutrino flavors, N_α, affects the equilibration and thermalization of quantum many-body neutrino systems. For our investigation, we utilize the full neutrino-neutrino Hamiltonian, as derived in Ref. [1], thereby including the usually neglected non-forward scattering terms. We then analyze several many-body neutrino systems with differing numbers of flavors, focusing on $N_\alpha \in \{1, 2\}$, and we examine the thermalization process for both flavor and momentum degrees of freedom. Our results suggest that a higher number of flavors will increase entanglement entropy and shorten the timescales required to achieve thermalization.

1 Introduction and Formalities

Neutrinos are charge-neutral, spin-1/2 particles, and are only known to interact via two forces, the weak force and the gravitational force [2]. Of the known, massive elementary particles, neutrinos are among the lightest and most abundant in the universe. They have extremely small masses and interact very weakly, yet they play a critical role in many dense astrophysical processes, such as core-collapse supernovae and neutron star mergers, where they are produced in vast quantities. For example, we can consider one of the closest supernovae in modern history, SN1987A, as discussed in Ref. [2], which occurred very near our own Milky Way galaxy, in the Large Magellanic Cloud, and which was carefully observed here on Earth on February 23, 1987. Roughly three hours before the resulting light from the explosion reached us here on Earth, a significant burst of neutrinos was detected in neutrino detectors around the world. It is expected that during a core-collapse supernovae, such as SN1987A, approximately 99% of the gravitational energy is converted into an extraordinary number of neutrinos; From the number of neutrinos detected during the event, it is estimated that the number of neutrinos released was on the order of 10^{58}, as was somewhat anticipated from previous attempts in modeling supernovae [2].

The creation and emission of such vast quantities of neutrinos is believed to be a key factor in the generation the outward shockwave that we then eventually see as a supernovae. Furthermore, these dense neutrino systems seem to be heavily involved in the creation of the heavier elements during such violent celestial events, in a process known as nucleosynthesis [2, 3]. Differences in how neutrino interactions are modeled can have a drastic effect on the simulations resulting abundance of various elements, as seen in Ref. [3]. As such, there is a significant interest in understanding how these resulting dense neutrino systems affect the overall astrophysical processes from which they have spawned. However, this is a monumental task, given the scale and complexity of such systems, so requires the use of some clever approximations.

As discussed in Refs. [1, 2], it is quite common to study astrophysical neutrinos through the use of Quantum Kinetic Equations (QKEs). The QKEs are time-evolution equations for the one-body reduced neutrino density matrix, which have been derived from quantum field theory using various methods. However, there is still the lingering question about the validity of this kind of one-body analysis, and if it leaves out any important many-body correlations or entanglement effects, especially in the context of quantum many-body approaches to the problem of the neutrino gas, as mentioned in Ref. [1].

It is our understanding that, until the very recent work done in Ref. [1], which derives the full neutrino-neutrino interaction Hamiltonian $H_{\nu\nu}$ from the Standard Model, studies on quantum many-body neutrino systems have used a truncated neutrino-neutrino interaction Hamiltonian $H^{(T)}_{\nu\nu}$, which neglects non-forward kinematics. As we can see in Ref. [1], results obtained using $H_{\nu\nu}$ do not necessarily line up with those obtained using $H^{(T)}_{\nu\nu}$. As such, it is imperative that we thoroughly investigate how these quantum many-body neutrino systems behave when using $H_{\nu\nu}$. For these reasons, this paper aims to investigate the equilibration and thermalization properties of these dense quantum many-body neutrino systems.

Please note that, for the sake of convenience, we use natural units throughout this paper (i.e. $\hbar = c = 1$). Additionally, for similar reasons, we represent our individual neutrinos as plane-waves.

1.1 Neutrino Oscillations

An important consideration when modeling neutrino dynamics is that of neutrino oscillations (vacuum oscillations). Neutrino oscillations occur because the neutrinos of definite flavor, ν_α, are

linear combinations of neutrino mass eigenstates, ν_m, of the vacuum term of the Hamiltonian, H_{vacuum} [4]. Effectively, this means that a neutrino that begins as some definite flavor, α, will gradually oscillate into being a superposition of several different neutrino flavors. After some amount of time, t, a neutrino which began as some initial flavor, α, would have the possibility to then be measured as a different flavor, say α'.

To demonstrate this effect, we can consider a single neutrino born with a definite flavor α. For the sake of simplicity, we can treat this neutrino as being a plane wave [4]. Following along with Kayser's discussion on neutrino oscillations in Ref. [4], the wavefunction of this neutrino at it's birth can be written as

$$\psi(x, t = 0) = \sum_m U_{\alpha m} \nu_m e^{ip_\nu x}, \tag{1}$$

where U is an orthonormal mixing matrix and p_ν is the fixed momentum of the neutrino. The time evolved wavefunction can then be written as

$$\psi(x, t) = \sum_m U_{\alpha m} \nu_m e^{ip_\nu x} e^{-iE_m(p_\nu)t}, \tag{2}$$

where $E_m(p_\nu)$ represents the energy associated with the mass eigenstate m and the momentum of the neutrino p_ν. Because neutrinos travel at hyper-relativistic speeds, we can assume that at time t, we will have that $x \approx t$. Additionally, because all of the masses M_m are much smaller than p_ν, we can use the approximation

$$E_m(p_\nu) \approx p_\nu + \frac{M_m^2}{2p_\nu}. \tag{3}$$

As further discussed by Kayser in Ref. [4], we can use these approximations to then rewrite the time evolved wavefunction as

$$\psi(t, t) \approx \sum_m U_{\alpha m} \nu_m e^{-i\frac{M_m^2}{2p_\nu}t}. \tag{4}$$

This expression allows us to easily show that the probability P of finding the neutrino as being flavor α' at some distance x away from it's source is

$$P = |\langle v_{\alpha'} \mid \psi(x, t)\rangle|^2 = \sum_m U_{\alpha' m}^2 U_{\alpha m}^2 + \sum_{m' \neq m} U_{\alpha' m} U_{\alpha m} U_{\alpha' m'} U_{\alpha m'} \cos\left(\frac{|M_m^2 - M_{m'}^2|}{2p_\nu} x\right), \tag{5}$$

which demonstrates to us that a neutrino which is born of some flavor α can oscillate into another flavor α', as desired.

In the results which we will be considering later, in Sect 2, we are currently neglecting vacuum oscillations, which allows us to conserve for total lepton flavor. In the very dense neutrino systems we are considering, the neutrino-neutrino interaction term, $H_{\nu\nu}$, is expected to dominate. However, we are planning to run future simulations that also consider vacuum oscillations, thereby allowing for the violation of lepton number conservation, to then compare with our current results.

1.2 The Hilbert Space

In an effort to formalize our quantum many-body neutrino systems, we begin by considering a system of neutrinos confined to a finite volume, V, which allows us to discretize the various one-body energy eigenstates, as well as allowing us to treat our various neutrinos as plane waves in said volume. We assume that there is some maximum one-body momentum mode number, k, that

the system will not exceed, due to the conservations of the energy and momentum of our N-body system. We can identify a particle by its three momentum $\mathbf{p}_i$, where $i \in \{1, 2, \cdots, k\}$, and by a flavor label α_j, where $j \in \{1, 2, \cdots, N_\alpha\}$ [1]. Throughout this paper, we are mainly considering systems of $N_\alpha = 2$ flavors, for which we will instead denote the flavor label as some $\alpha \in \{e, \mu\}$, for simplicity. Considering a system of N neutrinos, we can see that there is an upper limit on the dimension, d_h, of the Hilbert space of said system,

$$\max\left(d_h\right) = \binom{N_\alpha \times k}{N}. \tag{6}$$

However, this upper limit can be reduced by considering the consequences of conservation laws on the evolution of some initial state, such as the conservations of kinetic energy and momentum. The conservation of kinetic energy will be further discussed later on in Sect. 1.6. Additionally, in this paper, since we are currently neglecting the H_{vacuum} term, we can also enforce lepton flavor conservation, thereby further reducing the effective dimension of the Hilbert space of a given N-body neutrino system. Our current results, which are discussed in Sect 2, are all for an 8-body neutrino system with $N_\alpha = 2$ and $k = 35$, yet our largest effective Hilbert space has a dimension $d_h = 1260$, which allows us to simulate the full-body evolution of such systems by exactly diagonalizing the Hamiltonian.

1.3 Second Quantization

In order to further develop our model for quantum many-body neutrino systems, we utilize second quantization, as described in Refs. [1, 5]. Recognizing that neutrinos are fermions, we can see that for a system of N neutrinos, the wavefunction of our many-body basis state can be written using the Slater Determinant (denoted as "S.D."), as is done in Ref. [1], giving us

$$|\mathbf{n}\rangle = \text{S.D.}\left(\prod_{\alpha_j p_i:\ n_{\alpha_j p_i}=1} |\mathbf{p}_i, \alpha_j\rangle\right). \tag{7}$$

We can then represent our many-body basis states in the occupation number representation, taking the ordered set $\mathbf{n} = \{n_{\alpha_1 p_1}, n_{\alpha_2 p_1}, \cdots, n_{\alpha_{N_\alpha} p_1}, n_{\alpha_1 p_2}, \cdots, n_{\alpha_{N_\alpha} p_k}\}$ as being the occupation numbers for our single particle basis states, which allows us to write the many-body basis states in the form

$$|\mathbf{n}\rangle \doteq |n_{\alpha_1 p_1}, n_{\alpha_2 p_1}, \cdots, n_{\alpha_{N_\alpha} p_1}, n_{\alpha_1 p_2}, \cdots, n_{\alpha_{N_\alpha} p_k}\rangle, \tag{8}$$

where $n_{\alpha_j p_i} \in \{0, 1\}$.

We then introduce the annihilation and creation operators, $\hat{a}_{\alpha_j}(\mathbf{p}_i)$ and $\hat{a}^\dagger_{\alpha_j}(\mathbf{p}_i)$. Note that the annihilation and creation operators are Hermitian conjugates of each other. These operators act on functions in the occupation number basis and play a leading role in the method of second quantization [5]. By design, the annihilation operator $\hat{a}_{\alpha_j}(\mathbf{p}_i)$ decreases the value of the occupation number $n_{\alpha_j p_i}$ of an occupied state by unity, thereby causing it to become unoccupied. Conversely the creation operator $\hat{a}^\dagger_{\alpha_j}(\mathbf{p}_i)$ increases the value of the occupation number $n_{\alpha_j p_i}$ of an unoccupied state by unity, thereby causing it to become occupied. It is vital that we account for the anti-commutation of the creation and annihilation operators correctly, so we introduce an ordering rule for the basis $|\mathbf{n}\rangle$; The order of our occupied one-body basis states reflects their order in the ordered set $\mathbf{n}$, described above. This allows us to then rewrite the N-body basis states in the form

$$|\mathbf{n}\rangle \doteq \frac{\hat{a}^\dagger_{\alpha_{j_1}}(\mathbf{p}_{i_1})}{\sqrt{V}} \frac{\hat{a}^\dagger_{\alpha_{j_2}}(\mathbf{p}_{i_2})}{\sqrt{V}} \cdots \frac{\hat{a}^\dagger_{\alpha_{j_N}}(\mathbf{p}_{i_N})}{\sqrt{V}} |0\rangle, \tag{9}$$

where α_{j_n} and p_{i_n} are the flavor and momentum of the nth neutrino in a given N-body neutrino system [1]. The annihilation and creation operators are both proportional to $\sqrt{V}$, so we also multiply each operator by a factor of $\frac{1}{\sqrt{V}}$ to normalize our states. Notice that the complex conjugate of this general N-body basis state can be represented as

$$\langle \mathbf{n}| \doteq \langle 0| \frac{\hat{a}_{\alpha_{j_N}}(\mathbf{p}_{i_N})}{\sqrt{V}} \cdots \frac{\hat{a}_{\alpha_{j_2}}(\mathbf{p}_{i_2})}{\sqrt{V}} \frac{\hat{a}_{\alpha_{j_1}}(\mathbf{p}_{i_1})}{\sqrt{V}}. \tag{10}$$

These N-body basis states form an orthonormal basis and collectively form the largest possible Hilbert space for a given N-body neutrino system, which we discussed in Sect. 1.2. Using these basis states, we can represent a generic state in this Hilbert space by

$$|\Psi\rangle = \sum_{n}^{d_h} c_n |\mathbf{n}\rangle , \tag{11}$$

where c_n are complex amplitudes [1].

1.4 The Full Hamiltonian

Using this representation for our quantum many-body neutrino systems, we can now construct the Hamiltonian, as described in Ref. [1]. When restricting ourselves to two flavors of neutrino, representing our flavor label as $\alpha \in \{e, \mu\}$, we can write the kinetic term of the Hamiltonian as

$$\begin{aligned} H_{\text{kin}} = \int \frac{d\mathbf{p}}{(2\pi)^3} \Bigg[& \left(|\mathbf{p}| + \frac{M_1^2 + M_2^2 - \cos(2\theta)\ \delta M^2}{4|\mathbf{p}|} \right) \hat{a}_e^\dagger(\mathbf{p}) \hat{a}_e(\mathbf{p}) \\ & + \left(|\mathbf{p}| + \frac{M_1^2 + M_2^2 + \cos(2\theta)\ \delta M^2}{4|\mathbf{p}|} \right) \hat{a}_\mu^\dagger(\mathbf{p}) \hat{a}_\mu(\mathbf{p}) \\ & + \frac{\sin(2\theta)\ \delta M^2}{4|\mathbf{p}|} \left(\hat{a}_e^\dagger(\mathbf{p}) \hat{a}_\mu(\mathbf{p}) + \hat{a}_\mu^\dagger(\mathbf{p}) \hat{a}_e(\mathbf{p}) \right) \Bigg], \end{aligned} \tag{12}$$

where M_m are the masses of the neutrino mass eigenstates and where $\delta M^2 = M_2^2 - M_1^2$. Notice that the last term is the usual vacuum mixing term.

The full neutrino-neutrino interaction term of the Hamiltonian can be written as

$$\begin{aligned} H_{\nu\nu} = & \frac{G_F}{\sqrt{2}} \sum_{\alpha,\alpha',\beta,\beta'} \int \frac{d\mathbf{q}}{(2\pi)^3} \frac{d\mathbf{q}'}{(2\pi)^3} \frac{d\mathbf{p}}{(2\pi)^3} \frac{d\mathbf{p}'}{(2\pi)^3} (2\pi)^3 \delta(\mathbf{p} + \mathbf{q} - \mathbf{p}' - \mathbf{q}') \\ & \times \left(\hat{a}_{\alpha'}^\dagger(\mathbf{p}') \hat{a}_\alpha(\mathbf{p}) \hat{a}_{\beta'}^\dagger(\mathbf{q}') \hat{a}_\beta(\mathbf{q}) \frac{\delta_{\alpha'\alpha}\delta_{\beta'\beta} + \delta_{\alpha'\beta}\delta_{\beta'\alpha}}{2} g(\mathbf{p}', \mathbf{p}, \mathbf{q}', \mathbf{q}) \right), \end{aligned} \tag{13}$$

with

$$g(\mathbf{p}', \mathbf{p}, \mathbf{q}', \mathbf{q}) = f^\dagger(\mathbf{p}', \mathbf{q}')\ f(\mathbf{p}, \mathbf{q}), \tag{14}$$

$$f(\mathbf{p}, \mathbf{q}) = \sqrt{2} \left(e^{-i\phi_{\mathbf{p}}} \sin\left(\frac{\theta_{\mathbf{p}}}{2}\right) \cos\left(\frac{\theta_{\mathbf{q}}}{2}\right) - e^{-i\phi_{\mathbf{q}}} \cos\left(\frac{\theta_{\mathbf{p}}}{2}\right) \sin\left(\frac{\theta_{\mathbf{q}}}{2}\right) \right), \tag{15}$$

where the factor G_F is the Fermi constant, the factor $\delta(\mathbf{p} + \mathbf{q} - \mathbf{p}' - \mathbf{q}')$ accounts for conservation of momentum, and the factor $g(\mathbf{p}', \mathbf{p}, \mathbf{q}', \mathbf{q})$ uses the relative angles of the momenta involved in a given neutrino-neutrino interaction to account for the strength of the interaction. Note that we use the spherical coordinates $\phi_{\mathbf{p}}$, $\theta_{\mathbf{p}}$, $\phi_{\mathbf{q}}$, and $\theta_{\mathbf{q}}$ to represent the directions of $\mathbf{p}$ and $\mathbf{q}$, respectively. As we can see, the Hamiltonian also uses the annihilation and creation operators, to annihilate the momenta that we started with and create the momenta that we end with, for a given interaction.

1.5 Setup for Hot and Dense Media

As is done if Ref. [1], it is now useful to consider and discuss the energy scales which characterize the dynamics of many-body neutrino systems of astrophysical interest, and then define a rescaled, dimensionless Hamiltonian. For neutrinos systems of astrophysical interest, the initial state is not too far from equilibrium, so in an effort to estimate the relative sizes of the various contributions to the Hamiltonian H, we assume an approximately valid scaling relation between the system's temperature T, volume V, and number of neutrinos N by $1/V \sim T^3/N$. Since the temperatures of the systems we are considering are at least of order MeV, the energy scales will be separated by many orders of magnitude, meaning

$$|\mathbf{p}| \sim T \gg G_F T^3 \gg \frac{\delta M^2}{T}. \tag{16}$$

For the situations we are considering, the scales of T and $G_F T^3$ differ by about ten orders of magnitude, while $G_F T^3$ and $\delta M^2/T$ differ by another two or three order of magnitude, depending on the magnitude of the mass splitting used [1].

Continuing with the process described in Ref. [1], we consider a unit of energy (and inverse time) defined by the quantity $\mathcal{E} \equiv G_F/(\sqrt{2}V)$ and we introduce the dimensionless parameters

$$\bar{T} = \frac{T}{\mathcal{E}} \sim 10^{10} \tag{17}$$

$$\bar{\omega} = \frac{\delta M^2}{4T\mathcal{E}} \sim 10^{-3} - 10^{-2} \tag{18}$$

$$|\tilde{\mathbf{p}}| = \frac{|\mathbf{p}|}{T} \sim O(1), \tag{19}$$

which then allows us to rewrite the Hamiltonian in the following way:

$$H = \mathcal{E}\left(\bar{H}_{\text{kin}} + \bar{H}_{\nu\nu}\right)$$

$$\begin{aligned}\bar{H}_{\text{kin}} = \frac{1}{V}\sum_{i=1}^{k}&\left(\bar{T}|\tilde{\mathbf{p}}_i| - \frac{\bar{\omega}\cos(2\theta)}{|\tilde{\mathbf{p}}_i|}\right)\hat{a}_e^\dagger(\mathbf{p}_i)\hat{a}_e(\mathbf{p}_i) + \left(\bar{T}|\tilde{\mathbf{p}}_i| + \frac{\bar{\omega}\cos(2\theta)}{|\tilde{\mathbf{p}}_i|}\right)\hat{a}_\mu^\dagger(\mathbf{p}_i)\hat{a}_\mu(\mathbf{p}_i) \\ &+ \frac{\bar{\omega}\sin(2\theta)}{|\tilde{\mathbf{p}}_i|}\left[\hat{a}_e^\dagger(\mathbf{p}_i)\hat{a}_\mu(\mathbf{p}_i) + \hat{a}_\mu^\dagger(\mathbf{p}_i)\hat{a}_e(\mathbf{p}_i)\right]\end{aligned} \tag{20}$$

$$\bar{H}_{\nu\nu} = -\frac{1}{V^2}\sum_{i,j,k,l} g(\mathbf{p}_i,\mathbf{p}_j,\mathbf{p}_k,\mathbf{p}_l)\ \delta(\mathbf{p}_i+\mathbf{p}_j-\mathbf{p}_k-\mathbf{p}_l)\ \hat{a}_\alpha^\dagger(\mathbf{p}_i)\hat{a}_\beta^\dagger(\mathbf{p}_j)\hat{a}_\alpha(\mathbf{p}_k)\hat{a}_\beta(\mathbf{p}_l).$$

For the systems we will be discussing in Sect. 2, we will be neglecting the H_{kin} term of the Hamiltonian and only consider the effects of the $H_{\nu\nu}$ term. In the hot, dense astrophysical environments that we are interested in, and over the incredibly short time scales that we are considering, we expect that the effects from the $H_{\nu\nu}$ term will be far greater than the effects from the vacuum oscillations part of the H_{kin} term. In addition, we approximately have that kinetic energy is conserved, as we will discuss in the next section, Sect. 1.6. However, there are plans to include the H_{kin} term in future simulations, as is later discussed in Sect. 3.

1.6 Conservation of Kinetic Energy

As a result of considering such hot and dense astrophysical scales, with $\bar{T} \sim 10^{10}$, we can further simplify our many-body neutrino systems by noticing an interesting relationship between $\bar{T}$ and the conservation of kinetic energy [1]. In Fig. 1, it can been observed that dense neutrino systems with high $\bar{T}$ will have a strong tendency to conserve their kinetic energy. Therefore, we will enforce kinetic energy conservation, allowing us to further rewrite the neutrino-neutrino interaction term of the Hamiltonian as

$$\begin{aligned} \bar{H}^{(K)}_{\nu\nu} = &- \frac{1}{V^2} \sum_{i,j,k,l} \hat{a}^\dagger_\alpha(\mathbf{p}_i)\hat{a}^\dagger_\beta(\mathbf{p}_j)\hat{a}_\alpha(\mathbf{p}_k)\hat{a}_\beta(\mathbf{p}_l) \\ &\times \delta(\mathbf{p}_i + \mathbf{p}_j - \mathbf{p}_k - \mathbf{p}_l)\ \delta(|\mathbf{p}_i| + |\mathbf{p}_j| - |\mathbf{p}_k| - |\mathbf{p}_l|)\ g(\mathbf{p}_i, \mathbf{p}_j, \mathbf{p}_k, \mathbf{p}_l). \end{aligned} \tag{21}$$

This is the Hamiltonian that we use in the simulations which are discussed in the next section, Sect. 2.

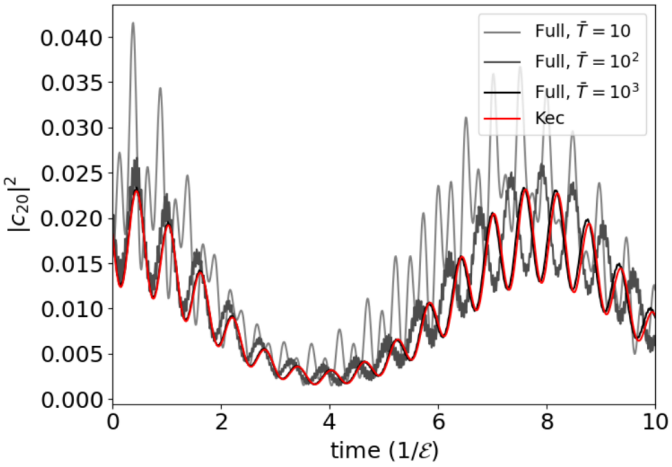

Figure 1: The squared modulus of the amplitude of the 20th basis state simulate with $H_{\nu\nu}$ (denoted as "Full") and with $H^{(K)}_{\nu\nu}$ (denoted as "Kec"). The Hamiltonian parameters are $\overline{\omega} = 1.0$ and $\sin(2\theta) = 0.8$. The model has $k = 11$ momentum modes, and $N = 2$ neutrinos. Note that the black solid line is almost on top of the red solid line. Credit: Vincenzo Cirigliano, Srimoyee Sen, and Yukari Yamauchi. "Neutrino many-body flavor evolution: the full Hamiltonian". see Ref. [1].

2 Results and Discussion

2.1 Initial Conditions

Before we dive into the results of our simulations, it is important to first understand the context of each of the systems we will be looking at. As discussed previously, we are going to be investigating 8-body neutrino systems. For our simulations, we consider systems with momentum modes on a two-dimensional grid and we introduce a "UV" cut-off p_{max} that determines the maximum magnitude of the momenta. In an effort to mimic astrophysical situations in which there is a net flux of neutrinos, we also only consider momentum modes with a positive x component, as is also

done in Ref. [1]. We can write this as

$$\begin{aligned} \tilde{\mathbf{p}}_i &\equiv \frac{\mathbf{p}_i}{T} = \frac{2\pi}{LT}\mathbf{z}_i \ , \\ \mathbf{z}_i &\in \{(z_x, z_y);\ \text{such that}\ z_x, z_y \in \mathbb{Z}, 0 < |\mathbf{z}_i| \leq z_{max},\ \text{and}\ 0 < z_x\}. \end{aligned} \tag{22}$$

For our simulations we take $z_{\max} = 5$, which gives us $k = 35$ total momentum modes to choose from. However, given our choice of initial conditions, conservations laws will cause all of our systems to only visit 18 of the available momentum modes. We label the momentum modes in an increasing order of z_y and z_x. For our simulations we chose the momentum modes

$$\begin{aligned} \mathbf{z}_6 = (3,-3), \mathbf{z}_9 = (2,-2), \mathbf{z}_{11} = (4,-2), \mathbf{z}_{13} = (2,-1), \\ \mathbf{z}_{21} = (1,1), \mathbf{z}_{26} = (2,2), \mathbf{z}_{27} = (3,2),\ \text{and}\ \mathbf{z}_{29} = (1,3), \end{aligned} \tag{23}$$

as depicted by the left grid in Fig. 2. Furthermore, for these simulations, we are only varying the neutrino flavors, from $(N_e, N_\mu) = (8, 0)$, to a maximal mixing of of the number of flavors, $(N_e, N_\mu) = (4, 4)$.

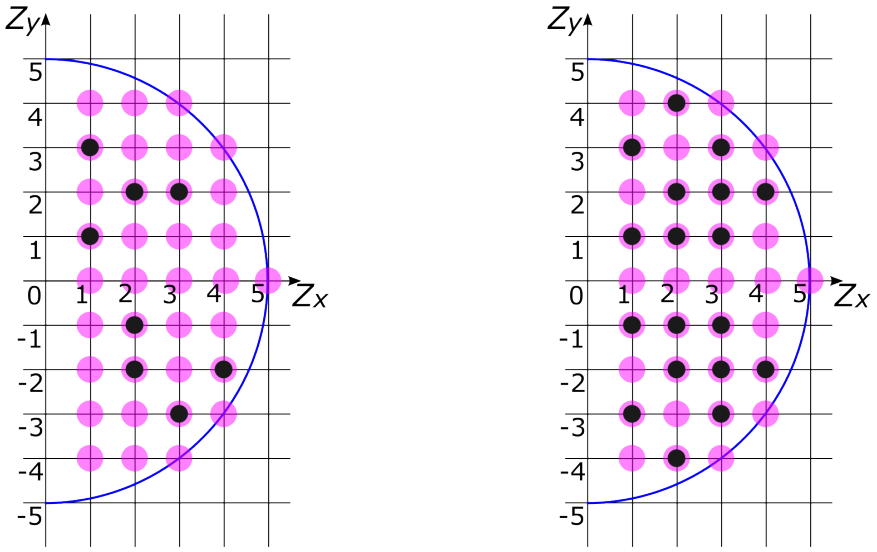

Figure 2: The left grid shows the initially occupied momentum modes, marked with black dots, for all of the 8-body neutrino systems we consider. The right grid shows all of the momentum modes that are visited by all of the time evolved 8-body neutrino systems we consider. In both graphs, all $k = 35$ momentum modes are marked in pink.

2.2 One-Body Observables $N_i^+ N$

As is done in Ref. [1], we use the reduced one-body density operator $\rho^{(1)}_{\alpha\beta}$ to define the one-body observables $N_i^+ N$ via the operator N_i^+, which represents the total occupation number for momentum mode $\mathbf{p}_i$ (normalized to N), as follows:

$$\rho^{(1)}_{\alpha\beta}(\mathbf{p}_i) = \frac{1}{N} \langle \Psi | \frac{\hat{a}^\dagger_\beta(\mathbf{p}_i)}{\sqrt{V}} \frac{\hat{a}_\alpha(\mathbf{p}_i)}{\sqrt{V}} | \Psi \rangle \ , \tag{24}$$

$$N_i^+ = \rho^{(1)}_{ee}(\mathbf{p}_i) + \rho^{(1)}_{\mu\mu}(\mathbf{p}_i). \tag{25}$$

We then use these one-body observables to study the kinetic properties of our quantum 8-body neutrino systems, under time evolution. We started with a system of $(N_e, N_\mu) = (8, 0)$ neutrinos, where all initial momenta modes are occupied by e flavored neutrinos. And then for each successive simulation, we altered our system by changing the initial flavors, such that the flavor of the highest indexed momentum mode $\mathbf{z}_i$ that is occupied by an e flavored neutrino is changed to a μ flavored neutrino, until we had a maximal mixing of flavors, $(N_e, N_\mu) = (4, 4)$. We can see the results of most of this process in Fig. 3.

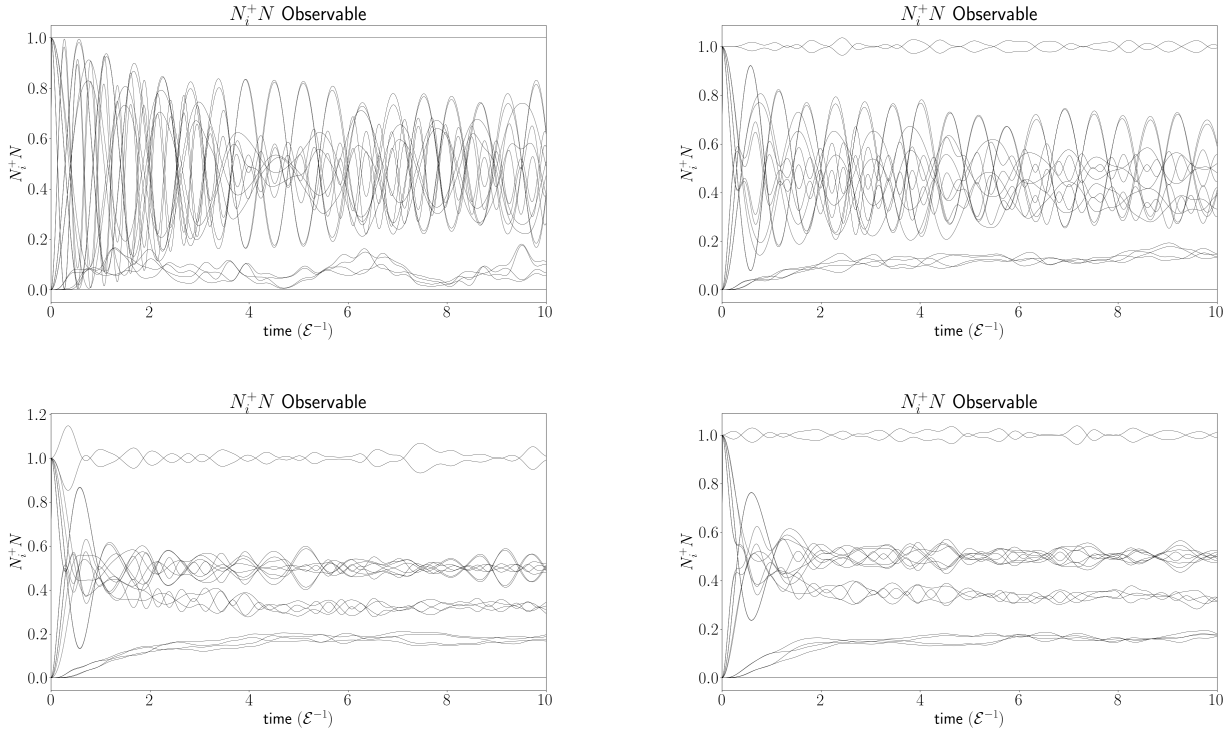

Figure 3: Time evolved N_i^+N observables for four different 8-body neutrino systems. Each system occupies the same initial momentum modes. They differ from each other by the number of electron neutrinos N_e and the number of muon neutrinos N_μ in the system. We start with all of the initial momenta occupied by e flavored neutrinos, and then we progressively change the initial flavors, such that the flavor of the highest indexed momentum mode $\mathbf{z}_i$ occupied by an e flavored neutrino is changed to a μ flavored neutrino. Top left: $(N_e, N_\mu) = (8, 0)$, with $d_h = 14$. Top right: $(N_e, N_\mu) = (7, 1)$, with $d_h = 126$. Bottom left: $(N_e, N_\mu) = (6, 2)$, with $d_h = 476$. Bottom right: $(N_e, N_\mu) = (5, 3)$, with $d_h = 994$.

As we can see in Fig. 3, in the case where $(N_e, N_\mu) = (8, 0)$ there is practically no convergence to a steady state. When we replace a single electron neutrino with a muon neutrino, in the case where $(N_e, N_\mu) = (7, 1)$, we still don't really see much convergence; However, notice that in the central group of curves, there appear to be two smaller sub groups of curves that diverge from each other. In the case where $(N_e, N_\mu) = (6, 2)$, we can clearly see that our system is now converging to some steady state, which further improves in the $(N_e, N_\mu) = (5, 3)$ case.

Further following our process for choosing which initial flavors occupy which initial momentum mode, as we described above, when we have $(N_e, N_\mu) = (4, 4)$, we end up with the left graph in Fig. 4, showing us that our new system doesn't converge as cleanly towards a steady state, compared to

the $(N_e, N_\mu) = (5, 3)$ system. In an attempt to further explore the effect that our initial conditions have on our $(N_e, N_\mu) = (4, 4)$ system, we alter which flavors α occupy which initial momentum modes $\mathbf{p}_i$, from having the initial e flavored neutrinos occupying the modes $\mathbf{z}_6, \mathbf{z}_9, \mathbf{z}_{11}$, and $\mathbf{z}_{13}$, with the μ flavored neutrinos occupying the remaining initial momentum modes, to instead having the initial e flavored neutrinos occupy the modes $\mathbf{z}_6, \mathbf{z}_9, \mathbf{z}_{21}$, and $\mathbf{z}_{26}$. Doing this results in a much finer convergence towards some steady state, as can be seen by the right graph in Fig. 4. Both of these $(N_e, N_\mu) = (4, 4)$ systems share the exact same effective Hilbert space, of dimension $d_h = 1260$, so this difference is quite unexpected and will require further investigation.

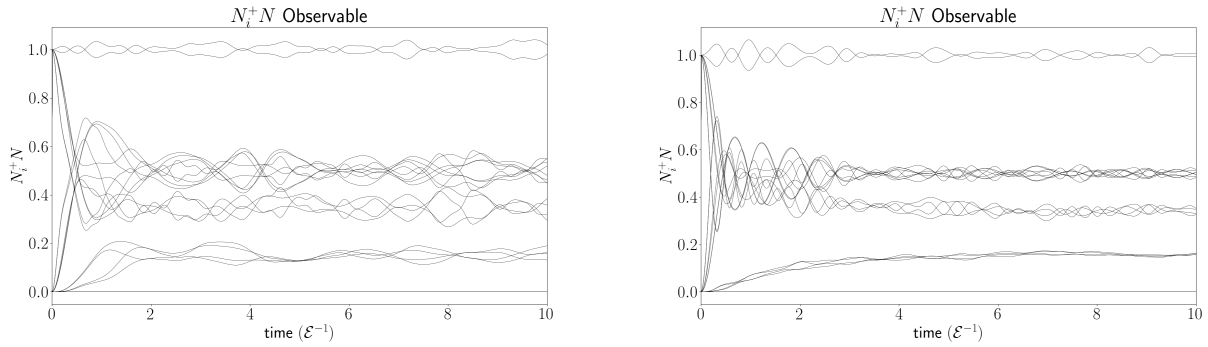

Figure 4: Time evolved N_i^+N observables for two different 8-body neutrino systems. Each system occupies the same initial momentum modes and has the same number of each neutrino flavor, $N_e = 4$ and $N_\mu = 4$. The two initial conditions differ only by which flavor of neutrino occupies each of the initial momentum modes. Both systems share the same exact Hilbert space, with $d_h = 1260$. Left graph: Initial e flavored neutrinos occupy modes $\mathbf{z}_6, \mathbf{z}_9, \mathbf{z}_{11}$, and $\mathbf{z}_{13}$, while the μ flavored neutrinos occupy the remaining modes. Right graph: Initial e flavored neutrinos occupy modes $\mathbf{z}_6, \mathbf{z}_9, \mathbf{z}_{21}$, and $\mathbf{z}_{26}$, while the μ flavored neutrinos occupy the remaining modes.

2.3 Microcanonical Ensemble

It is now useful to introduce the microcanonical ensemble for the quantum many-body neutrino systems we are studying. The microcanonical ensemble is a statistical tool we can use to find the expected values of observables $\mathcal{O}$ of our dense neutrino systems when they are in equilibrium, which we calculate using the formula $\mathrm{Tr}[\rho_{\mathrm{mc}}\mathcal{O}]$, where ρ_{mc} is the density operator for the microcanonical ensemble [1]. Since each of the many-body basis states $|\mathbf{n}\rangle$ in our systems of interest all have the same number of each flavor of neutrino, N_e and N_μ, as well as the same total energy, they are all equally probable in a microcanonical ensemble. Thus, we can write the corresponding density operator as

$$\rho_{\mathrm{mc}} = \frac{1}{d_h} \sum_{\mathbf{n}=1}^{d_h} |\mathbf{n}\rangle \langle \mathbf{n}| \,. \tag{26}$$

We then use this density operator calculate the equilibrium expectation values of the N_i^+N observables of our neutrino systems [1]:

$$\mathrm{Tr}[\rho_{\mathrm{mc}} N_i^+ N] = \frac{1}{d_h} \sum_{\mathbf{n}=1}^{d_h} \langle \mathbf{n}| N_i^+ |\mathbf{n}\rangle \,. \tag{27}$$

We found that the equilibrium expectation values of the N_i^+N observables are the same for all of the different 8-body neutrino systems that we investigated, as can been observed in Fig.

5. We found this to be somewhat surprising, since each successive Hilbert space is significantly larger than the previous one, as we gradually transition from $(N_e, N_\mu) = (8, 0)$ to $(N_e, N_\mu) = (4, 4)$. Even more surprisingly, the expectation values for the $N_i^+ N$ observables of our time evolved 8-body systems seem to be converging to a few values that are slightly off from their equilibrium expectation values. This is much more obvious when we take the difference between the two sets of values, as seen in Fig. 6.

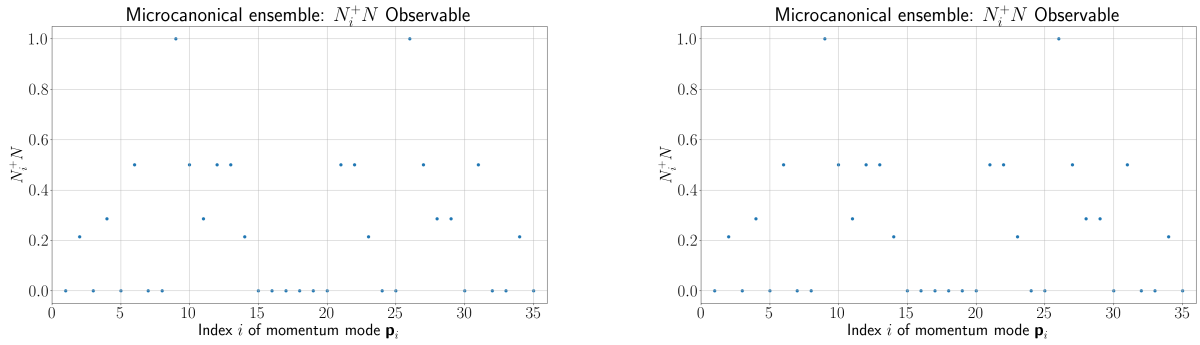

Figure 5: Microcanonical ensemble $N_i^+ N$ observables for our $N = 8$ neutrino system. Left graph: the number of allowed electron neutrinos and muon neutrinos are $N_e = 4$ and $N_\mu = 4$, respectively, resulting in a Hilbert space of size $d_h = 1260$. Right graph: the number of allowed electron neutrinos and muon neutrinos are $N_e = 8$ and $N_\mu = 0$, respectively, resulting in a Hilbert space of size $d_h = 14$.

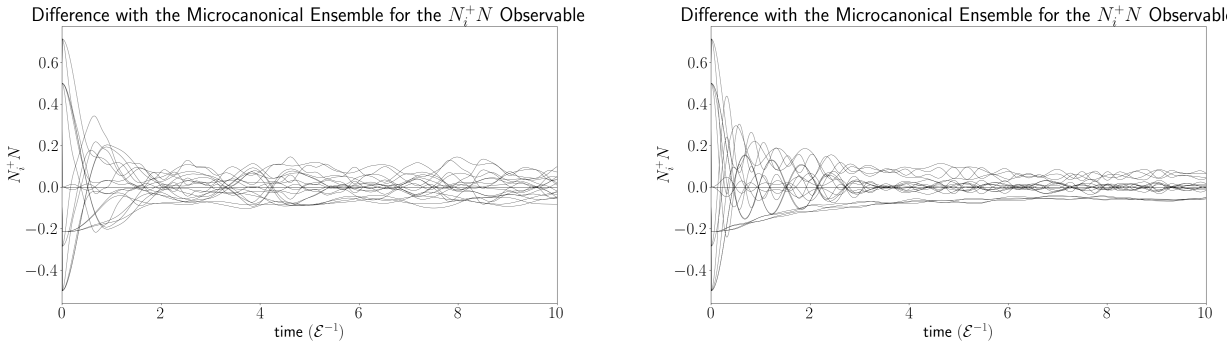

Figure 6: Difference between the microcanonical ensemble $N_i^+ N$ observables and the time evolved $N_i^+ N$ observables for two different 8-body neutrino systems. Each system occupies the same initial momentum modes and has the same number of each flavor, $N_e = 4$ and $N_\mu = 4$. Left graph: Initial e flavored neutrinos occupy modes $\mathbf{z}_6, \mathbf{z}_9, \mathbf{z}_{11}$, and $\mathbf{z}_{13}$, while the μ flavored neutrinos occupy the remaining modes. Right graph: Initial e flavored neutrinos occupy modes $\mathbf{z}_6, \mathbf{z}_9, \mathbf{z}_{21}$, and $\mathbf{z}_{26}$, while the μ flavored neutrinos occupy the remaining modes.

3 Future Work

There are still several open questions surrounding the results which we have explored above. First and foremost, we must further examine why we are not seeing a cleaner convergence towards the equilibrium expectation values of the $N^+ N$ observables, which we found using the microcanonical

ensemble. Additionally, the above results suggest that more work is needed to understand why our choice of initial conditions has such a drastic impact on how well our neutrino system converges. Indeed, it is clear the the next major step forward for this project is for us to further study the theoretical aspects of the thermalization/equilibration processes of these systems. To that end, we also plan to employ the use of more observables, such as those related to the flavor occupation numbers associated with each of the momenta of our systems, in future simulations.

Another important future step of this project is to investigate the case where we have three possible flavors of neutrinos, and where we gradually transition from a system of just a single neutrino flavor, to a system of two flavors, and then finally to a system which allows for all three flavors, while accounting for total flavor conservation of the system. If time permits, it may also be useful to explore systems with even more neutrino flavors, such as four or five flavors.

Finally, it is important to recognize that all of our current results were obtained using only the neutrino-neutrino interaction term of the Hamiltonian, $H_{\nu\nu}$, and that we neglected all other terms, such as the vacuum oscillation term, H_{vacuum}. Although the $H_{\nu\nu}$ term is expected to dominate in a dense neutrino gas, there are still going to be vacuum oscillations which may have some impact on our thermalization processes. Including vacuum oscillations would allow for our dense neutrino systems to violate total flavor conservation, thereby drastically increase the size of their respective Hilbert spaces. Therefore, another important future step of this project is to include those other terms to compare with the results which we have obtained thus far.

Acknowledgment

This research was supported by the INT's U.S. Department of Energy grant No. DE-FG02-00ER41132 and the N3AS's National Science Foundation award No. 2020275.

References

[1] Vincenzo Cirigliano, Srimoyee Sen, and Yukari Yamauchi. "Neutrino many-body flavor evolution: the full Hamiltonian". In: *Phys. Rev. D* 110 (12 Dec. 2024), p. 123028. DOI: 10.1103/PhysRevD.110.123028. arXiv: 2404.16690 [hep-ph].

[2] M. Cristina Volpe. "Neutrinos from dense environments: Flavor mechanisms, theoretical approaches, observations, and new directions". In: *Rev. Mod. Phys.* 96 (2 June 2024), p. 025004. DOI: 10.1103/RevModPhys.96.025004. URL: https://link.aps.org/doi/10.1103/RevModPhys.96.025004.

[3] A. Baha Balantekin et al. "Collective neutrino oscillations and heavy-element nucleosynthesis in supernovae: exploring potential effects of many-body neutrino correlations". In: (2024). arXiv: 2311.02562 [astro-ph.HE].

[4] Boris Kayser. "On the quantum mechanics of neutrino oscillation". In: *Phys. Rev. D* 24 (1 July 1981), pp. 110–116. DOI: 10.1103/PhysRevD.24.110. URL: https://link.aps.org/doi/10.1103/PhysRevD.24.110.

[5] Lev Davidovich Landau and E. M. Lifshits. *Quantum Mechanics: Non-Relativistic Theory*. Vol. 3. Course of Theoretical Physics. Oxford: Butterworth-Heinemann, 1991. ISBN: 978-0-7506-3539-4. DOI: 10.1016/C2013-0-02793-4.